

## PDF hosted at the Radboud Repository of the Radboud University Nijmegen

The following full text is a publisher's version.

For additional information about this publication click this link.

<http://hdl.handle.net/2066/98227>

Please be advised that this information was generated on 2017-12-06 and may be subject to change.

Published in final edited form as:

*Mol Imaging*. 2011 April ; 10(2): 144–152.

## Preclinical Evaluation of <sup>68</sup>Ga-DOTA-Minigastrin for the Detection of Cholecystokinin-2/Gastrin Receptor–Positive Tumors

Maarten Brom, Lieke Joosten, Peter Laverman, Wim J.G. Oyen, Martin Béhé, Martin Gotthardt, and Otto C. Boerman

Department of Nuclear Medicine, Radboud University Nijmegen Medical Centre, Nijmegen, The Netherlands, and the Division of Nuclear Medicine and PET Center, University Hospital of Freiburg, Freiburg, Germany

### Abstract

In comparison to somatostatin receptor scintigraphy, gastrin receptor scintigraphy using <sup>111</sup>In-DTPA-minigastrin (MG0) showed added value in diagnosing neuroendocrine tumors. We investigated whether the <sup>68</sup>Ga-labeled gastrin analogue DOTA-MG0 is suited for positron emission tomography (PET), which could improve image quality. Targeting of cholecystokinin-2 (CCK<sub>2</sub>)/gastrin receptor–positive tumor cells with DOTA-MG0 labeled with either <sup>111</sup>In or <sup>68</sup>Ga in vitro was investigated using the AR42J rat tumor cell line. Biodistribution was examined in BALB/c nude mice with a subcutaneous AR42J tumor. In vivo PET imaging was performed using a preclinical PET–computed tomographic scanner. DOTA-MG0 showed high receptor affinity in vitro. Biodistribution studies revealed high tumor uptake of <sup>68</sup>Ga-DOTA-MG0: 4.4 ± 1.3 %ID/g at 1 hour postinjection. Coadministration of an excess unlabeled peptide blocked the tumor uptake (0.7 ± 0.1 %ID/g), indicating CCK<sub>2</sub>/gastrin receptor–mediated uptake (*p* = .0005). The biodistribution of <sup>68</sup>Ga-DOTA-MG0 was similar to that of <sup>111</sup>In-DOTA-MG0. Subcutaneous and intraperitoneal tumors were clearly visualized by small-animal PET imaging with 5 MBq <sup>68</sup>Ga-DOTA-MG0. <sup>111</sup>In- and <sup>68</sup>Ga-labeled DOTA-MG0 specifically accumulate in CCK<sub>2</sub>/gastrin receptor–positive AR42J tumors with similar biodistribution apart from the kidneys. AR42J tumors were clearly visualized by microPET. Therefore, <sup>68</sup>Ga-DOTA-MG0 is a promising tracer for PET imaging of CCK<sub>2</sub>/gastrin receptor–positive tumors in humans.

Somatostatin receptor scintigraphy (SRS) is the standard procedure for the detection of neuroendocrine tumors (NETs) and their metastases.<sup>1,2</sup> The method is based on the specific binding of radio-peptides mainly to the somatostatin subtype 2 receptor, which is overexpressed on these tumors.<sup>3</sup> However, for some tumor types, the sensitivity of SRS is limited. For example, the detection rate of medullary thyroid carcinoma (MTC) with SRS is only 40%.<sup>4</sup> However, a tumor detection rate of 94% was observed with gastrin receptor scintigraphy with <sup>111</sup>In-DGlu<sup>1</sup>-minigastrin in patients with MTC, and when gastrin receptor scintigraphy was combined with computed tomography (CT), even 97% of the known tumor sites were detected.<sup>4</sup> Gotthardt and colleagues showed that gastrin receptor scintigraphy also had added value in patients with gastroenteropancreatic neuroendocrine tumors (GEP-NETs), especially when no or low uptake of <sup>111</sup>In-labeled octreotide was observed.<sup>5</sup> The principle of gastrin receptor scintigraphy is based on binding of radiolabeled minigastrin to

the cholecystokinin-2 (CCK<sub>2</sub>)/gastrin receptor, which is expressed on the majority of NETs and MTCs.<sup>6</sup>

Positron emission tomography (PET) is advantageous over conventional scintigraphy and single-photon emission computed tomography (SPECT) because of its excellent sensitivity in combination with its improved spatial resolution. A recent study in patients with NET showed that PET imaging with the somatostatin analogue <sup>68</sup>Ga-DOTA-TOC had a higher detection rate compared to conventional SRS.<sup>7</sup> Based on these findings, it might be possible to further improve the image quality and sensitivity of gastrin receptor scintigraphy by radiolabeling of MG0 with <sup>68</sup>Ga for PET imaging. Because <sup>68</sup>Ga is a generator-produced positron emitter, it is readily available—also in centers without a cyclotron—and relatively cheap.

In this study, we investigated the potential of <sup>68</sup>Ga-labeled DOTA-DGlu-(Glu)<sub>5</sub>-minigastrin (DOTA-MG0) for detection of CCK<sub>2</sub>/gastrin receptor-positive tumors in vitro using CCK<sub>2</sub>/gastrin receptor-positive AR42J cells and in vivo in a BALB/c nude mouse model with subcutaneous or intraperitoneal AR42J tumors. <sup>111</sup>In-DOTA-MG0 was used as a reference in this study.

## Materials and Methods

### Peptides and Radionuclides

DOTA-MG0 was obtained from Peptide Specialty Laboratories (PSL GmbH, Heidelberg, Germany). The gastrin analogue DOTA-(His)<sub>2</sub>-minigastrin<sup>8</sup> was obtained from Pi-Chem (Graz, Austria). The amino acid sequences of DOTA-MG0 and DOTA-(His)<sub>2</sub>-minigastrin are depicted in Table 1. <sup>111</sup>InCl<sub>3</sub> was obtained from Covidien (Petten, The Netherlands). <sup>68</sup>GaCl<sub>3</sub> was eluted from a TiO<sub>2</sub>-based 1,110 MBq <sup>68</sup>Ge/<sup>68</sup>Ga generator (obtained from IDB Holland BV originating from Obninsk, Russia) with 5 mL 0.1 N Ultrapure HCl (J.T. Baker, Deventer, The Netherlands). The <sup>68</sup>GaCl<sub>3</sub> was collected in five fractions of 1 mL; the second fraction containing the majority of <sup>68</sup>GaCl<sub>3</sub> was used for radiolabeling.

### Radiolabeling of DOTA-MG0 with <sup>111</sup>In

DOTA-MG0 was dissolved in 0.25 M ammonium acetate buffer, pH 5.5, 11 MBq <sup>111</sup>InCl<sub>3</sub> was added to 1 µg (0.5 nmol) peptide, and five volumes of 0.25 M ammonium acetate buffer, pH 5.5, were added containing 35 mM DL-methionine (Sigma Chemicals, St. Louis, MO) to prevent oxidation of the methionine residue. After 30 minutes' incubation at 95°C, 10 mM ethylenediaminetetraacetic acid (EDTA) was added to a final concentration of 1 mM. Quality control was performed using reversed-phase high-performance liquid chromatography (RP-HPLC) with a C<sub>18</sub> reversed-phase column (Zorbax Rx-C18; 4.6 × 250 mm; Agilent Technologies, Amstelveen, The Netherlands). The column was eluted with 0.1% trifluoroacetic acid (TFA) (Lab-scan, Analytical Sciences, Brussels, Belgium) in H<sub>2</sub>O with a linear gradient to 100% acetonitrile containing 0.1% TFA over 10 minutes with a flow of 1 mL/min. Instant thin-layer chromatography (ITLC) was performed on silica gel ITLC (ITLC-SG, Pall Corporation Life Sciences, New York, NY). Two mobile phases were used: 0.1 M EDTA in 0.1 M NH<sub>4</sub>Ac, pH 5.5 (R<sub>f</sub> <sup>111</sup>In-DOTA-MG0 = 0, R<sub>f</sub> <sup>111</sup>In-EDTA = 1) and 0.25 M NH<sub>4</sub>Ac, pH 5.5:methanol (1:1) (R<sub>f</sub> colloidal compounds = 0, R<sub>f</sub> <sup>111</sup>In-DOTA-MG0 ≥ 0.2 and R<sub>f</sub> <sup>111</sup>In-EDTA = 1). <sup>111</sup>In-DOTA-MG0 was used for in vitro and in vivo experiments without further purification.

## Radiolabeling of DOTA-MG0 with $^{68}\text{Ga}$

Radiolabeling of DOTA-MG0 was performed in 2.5 M HEPES (4-(2-hydroxyethyl)-1-piperazineethanesulfonic acid) buffer (Sigma Chemicals).  $^{68}\text{GaCl}_3$  (300 MBq in 1 mL) was added to 120  $\mu\text{L}$  HEPES buffer containing 13  $\mu\text{g}$  (6.2 nmol) DOTA-MG0. The final pH of the reaction mixture was 3.0. After incubation at 95°C for 20 minutes, 10 mM EDTA was added to a final concentration of 1 mM. The reaction mixture was purified by RP-HPLC as described above, except ethanol was used instead of acetonitrile containing 0.1% TFA. The peak containing  $^{68}\text{Ga}$ -DOTA-MG0 (including the oxidized fraction) was collected and diluted with phosphate-buffered saline (PBS) containing 0.5% w/v bovine serum albumin (BSA) to a final ethanol concentration of less than 5% before injection into mice (injection volume 0.2 mL). The unincorporated  $^{68}\text{Ga}$  and the  $^{68}\text{Ga}$ -colloid content in the purified  $^{68}\text{Ga}$ -labeled DOTA-MG0 preparations were determined using ITLC as described above.

## Cell Culture

The AR42J rat pancreatic tumor cell line<sup>9,10</sup> was used in these studies. Cells were maintained in Dulbecco's Modified Eagle's Medium (DMEM) with 4.5 g/L D-glucose (Gibco, Invitrogen, Breda, The Netherlands) supplemented with 10% fetal calf serum and 1% penicillin-streptomycin in a humidified 5%  $\text{CO}_2$  atmosphere at 37°C. The cells were harvested by trypsinization with trypsin/EDTA.

## IC<sub>50</sub> Determination

The apparent 50% inhibitory concentration (IC<sub>50</sub>) of DOTA-MG0,  $^{nat}\text{In}$ -DOTA-MG0, and  $^{nat}\text{Ga}$ -DOTA-MG0 was determined using AR42J cells grown in six-well plates (approximately  $10^6$  cells/well).

DOTA-MG0 was labeled with  $^{nat}\text{In}$  by adding 23.7 nmol  $\text{InCl}_3$  (Merck, Darmstadt, Germany) in 26.2  $\mu\text{L}$  0.02 M HCl to 73.8  $\mu\text{L}$  0.25 M ammonium acetate pH 5.5 containing 4.7 nmol DOTA-MG0. The labeling mixture was incubated at 95°C for 30 minutes. Labeling with  $^{nat}\text{Ga}$  was carried out by adding 23.7 nmol  $\text{Ga}(\text{NO}_3)_3$  (Sigma Chemicals) in 6  $\mu\text{L}$  0.02 M HCl to 44  $\mu\text{L}$  0.25 M ammonium acetate pH 5.5 containing 4.7 nmol DOTA-MG0. The reaction mixture was incubated overnight at room temperature.

The cells were washed twice with PBS and incubated with 2 mL binding buffer (DMEM with 4.5 g/L D-glucose with 0.5% w/v BSA) at 37°C for 60 minutes.  $^{111}\text{In}$ -labeled DOTA-MG0 (60,000 dpm, 5–10 pmol in 100  $\mu\text{L}$  binding buffer) was added to the cells after addition of various amounts of unlabeled peptide ranging from 0.1 to 300 nM. After incubation at room temperature for 2 hours, the medium was removed and the cells were washed twice with PBS. The cells were harvested with a cotton swab, and the radioactivity associated with the cells was measured in a well-type gamma counter (Wallac 1480-Wizard, Perkin-Elmer, Boston, MA). Under these conditions, internalization may occur. We therefore describe the results of this competitive binding assay as “apparent IC<sub>50</sub>” values rather than IC<sub>50</sub>.

## Peptide Dose Escalation Study

Six- to 8-week-old male BALB/c nude mice (Taconic, Hudson, NY) were injected subcutaneously in the right flank with  $1 \times 10^7$  AR42J cells. When the tumor had a diameter of 2 to 5 mm, mice were randomly divided in groups of five mice each. To determine the optimal peptide dose of DOTA-MG0 for targeting AR42J tumors in this model, mice were injected intravenously with 370 kBq  $^{111}\text{In}$ -DOTA-MG0 and were coinjected with escalating amounts of unlabeled DOTA-MG0, resulting in final peptide doses ranging from 0.1 to 100  $\mu\text{g}/\text{mouse}$ . One hour after injection, the mice were euthanized, tumor and relevant tissues were dissected and weighed, and the radioactivity was measured in a gamma counter.

## Biodistribution Studies of $^{68}\text{Ga}$ -DOTA-MG0 and $^{111}\text{In}$ -DOTA-MG0

BALB/c nude mice with a subcutaneous AR42J tumor were injected intravenously with 370 kBq (0.25  $\mu\text{g}$ )  $^{68}\text{Ga}$ -labeled DOTA-MG0 or 185 kBq (0.25  $\mu\text{g}$ )  $^{111}\text{In}$ -labeled DOTA-MG0. A separate group of three mice was coinjected with an excess (25  $\mu\text{g}$ ) unlabeled DOTA-(His)<sub>2</sub>-minigastrin (a CCK<sub>2</sub>/gastrin receptor ligand that was available in relatively high amounts) to determine receptor-mediated uptake. The mice were euthanized 1 hour after injection by CO<sub>2</sub>/O<sub>2</sub> suffocation. Tumor and relevant tissues were dissected, weighed, and counted in a gamma counter. The injected dose per gram (%ID/g) was determined for each tissue.

## PET-CT Imaging of Mice with Subcutaneous Tumors

PET images were acquired of BALB/c nude mice with a subcutaneous AR42J tumor on the shoulder using a small-animal PET-CT scanner (Inveon, Preclinical Solutions, Siemens Medical Solutions USA, Inc., Knoxville, TN). The scanner has an axial field of view of 12.7 cm and a 1.4 mm full width at half maximum (FWHM) spatial resolution in images reconstructed using Fourier rebinning and filtered backprojection.<sup>11</sup> When the tumor had a diameter of 2 to 5 mm, the mice were injected intravenously with 5 MBq (1  $\mu\text{g}$ )  $^{68}\text{Ga}$ -DOTA-MG0. Mice were euthanized by CO<sub>2</sub>/O<sub>2</sub> suffocation; PET images were acquired during 30 minutes, and images were reconstructed by ordered subset expectation maximization (OSEM3D)/maximum a posteriori (MAP) reconstruction with the following parameters: 256  $\times$  256 matrix, 2 OSEM3D iterations, 18 MAP iterations, and a resolution of 0.075 mm uniform variance. CT images were acquired for anatomic correlation directly after PET imaging (spatial resolution 113  $\mu\text{m}$ , 80 kV, 500  $\mu\text{A}$ , exposure time 300 ms).

## PET-CT Imaging of Mice with Intraperitoneal Tumors

Intraperitoneal tumors were induced by intraperitoneal injection of  $1 \times 10^6$  AR42J cells (injection volume 50  $\mu\text{L}$ ) under isoflurane inhalation anesthesia. PET scans were acquired weekly after injection of 5 MBq  $^{68}\text{Ga}$ -DOTA-MG0 (peptide dose 1  $\mu\text{g}$ ), starting 2 weeks after injection of the cells. PET-CT images were acquired as described above. For CT contrast, mice were injected intraperitoneally with 250  $\mu\text{L}$  nonionic contrast medium (Optiray 300, Covidien, Petten, The Netherlands). When tumors were clearly visible on PET scans, mice were euthanized by CO<sub>2</sub>/O<sub>2</sub> suffocation and the abdomen was examined macroscopically for tumor growth. Tumor and relevant tissues were dissected, weighed, and counted in a gamma counter. The %ID/g was determined for each tissue.

## Results

### Radiolabeling

Radiolabeling of DOTA-MG0 with  $^{68}\text{Ga}$  resulted in a specific activity up to 30 GBq/ $\mu\text{mol}$  with a radiochemical purity > 99% after HPLC purification. Before HPLC purification, the fraction of unincorporated  $^{68}\text{Ga}$  was < 5% and the labeling mixture contained approximately 3%  $^{68}\text{Ga}$ -colloid, as determined by ITLC. The fraction of oxidized  $^{68}\text{Ga}$ -DOTA-MG0 was always less than 2% as determined by HPLC. Unbound  $^{68}\text{Ga}$  had a retention time of 3 minutes, whereas the oxidized peptide and radio-labeled native peptide had a retention time of 13.2 and 13.5 minutes, respectively (Figure 1).

For  $^{111}\text{In}$ -DOTA-MG0, specific activities up to 45 GBq/ $\mu\text{mol}$  were obtained with a radiochemical purity > 95%. The fraction of oxidized  $^{111}\text{In}$ -DOTA-MG0 was always less than 2% as determined by HPLC.

### IC<sub>50</sub> Determination

The results of the IC<sub>50</sub> determination are summarized in Figure 2. The apparent IC<sub>50</sub> of DOTA-MG0, <sup>nat</sup>In-DOTA-MG0, and <sup>nat</sup>Ga-DOTA-MG0 of CCK<sub>2</sub>/gastrin receptor on AR42J cells was 2.4 nM (95% confidence interval 1.6 to 3.4), 3.2 nM (95% confidence interval 2.6 to 3.9), and 1.8 nM (95% confidence interval 1.7 to 2.0), respectively.

### Peptide Dose Escalation Study

The effect of the peptide dose on tumor targeting was studied in BALB/c nude mice with subcutaneous AR42J tumors. The results are summarized in Figure 3. The MG0 peptide dose had a pronounced effect on uptake in the AR42J tumor: uptake decreased at higher peptide doses. Highest tumor uptake of DOTA-MG0 was observed when 0.1 μg peptide was administered: 7.0 ± 0.6 %ID/g at 1 hour postinjection. Administration of 0.3 μg DOTA-MG0 resulted in a significantly reduced tumor uptake: 4.7 ± 0.8 %ID/g (*p* < .001). At the 1 μg peptide dose, there was still specific uptake of MG0 in the tumor (4.2 ± 0.5 %ID/g), whereas nonspecific uptake was as low as 0.23 ± 0.01 %ID/g. Besides tumor uptake, high kidney uptake of <sup>111</sup>In-DOTA-MG0 was observed. This kidney uptake decreased at higher doses of DOTA-MG0.

### Biodistribution of <sup>68</sup>Ga-DOTA-MG0 and <sup>111</sup>In-DOTA-MG0

The biodistribution of <sup>68</sup>Ga-DOTA-MG0 and <sup>111</sup>In-DOTA-MG0 in BALB/c nude mice with subcutaneous AR42J tumors is summarized in Figure 4. High tumor uptake of <sup>68</sup>Ga-DOTA-MG0 was observed 1 hour post-injection (4.4 ± 1.3 ID/g). Coadministration of an excess of unlabeled peptide (DOTA-(His)<sub>2</sub>-minigastrin) blocked the tumor uptake (0.7 ± 0.1 %ID/g, *p* = .0005), indicating CCK<sub>2</sub>/gastrin-mediated tumor uptake. Specific uptake was also observed in the stomach (*p* < .0001). High uptake was observed in the kidneys for both <sup>111</sup>In- and <sup>68</sup>Ga-labeled DOTA-MG0, which could not be blocked by an excess unlabeled DOTA-(His)<sub>2</sub>-minigastrin.

The biodistribution of <sup>111</sup>In-DOTA-MG0 in BALB/c nude mice with a subcutaneous AR42J tumor was highly similar to that of <sup>68</sup>Ga-DOTA-MG0, although kidney retention was two times higher for <sup>68</sup>Ga-labeled MG0 (see Figure 4). The explanation for this remarkable finding is unknown. There was no significant difference in uptake in the tumor or relevant organs between <sup>68</sup>Ga-labeled and <sup>111</sup>In-labeled DOTA-MG0.

RP-HPLC purification of <sup>68</sup>Ga-DOTA-MG0 was necessary because elevated uptake in liver and spleen was observed (1.1 ± 0.4 and 2.9 ± 0.3 %ID/g, respectively) when unpurified <sup>68</sup>Ga-DOTA-MG0, containing minor amounts of <sup>68</sup>Ga-colloid, was injected.

### PET Imaging of Subcutaneous Tumors

Subcutaneous AR42J tumors, with a diameter of approximately 5 mm, were clearly visualized on PET images as early as 1 hour after intravenous injection of <sup>68</sup>Ga-DOTA-MG0 (Figure 5). Besides tumor uptake, pronounced uptake was also seen in the kidneys. The PET images were fused with CT for anatomic correlation.

### PET Imaging of Intraperitoneal Tumors

Intraperitoneal tumor growth was observed on the PET images 28 to 35 days after tumor cell inoculation. The weight of the visualized lesions ranged from 0.044 to 0.499 g (median weight 0.057 g). The tumor of 0.044 g (approximately 1 mm in diameter) was clearly visible (Figure 6, A–C). A larger tumor (0.45 g, approximately 10 mm in diameter) adjacent to the left kidney was visualized despite the high kidney uptake (Figure 6, D–F). In one mouse, an abscess adjacent to the tumor was observed macroscopically and by CT. There was no

uptake of  $^{68}\text{Ga}$ -DOTA-MG0 in the abscess, and the tumor adjacent to the abscess was clearly visualized (Figure 6, G–I).

## Discussion

Gastrin receptor scintigraphy was shown to have an excellent detection rate in patients with MTC.<sup>4</sup> Moreover, gastrin receptor scintigraphy had an additional value in patients with GEP-NETs, and additional lesions were detected with gastrin receptor scintigraphy when no or low uptake was observed with SRS.<sup>5</sup> Owing to its excellent sensitivity and higher resolution, PET is advantageous over conventional scintigraphy and SPECT. It was previously shown that PET imaging with  $^{68}\text{Ga}$ -DOTA-TOC is a very sensitive method for the detection of NET.<sup>7</sup> Given that the sensitivity and spatial resolution of PET are higher compared to those of SPECT, it is expected that PET imaging with  $^{68}\text{Ga}$ -labeled DOTA-MG0 could improve the detection rate of NET and MTC. In patients with MTC,  $^{68}\text{Ga}$ -DOTA-MG0 PET might be the first choice over  $^{68}\text{Ga}$ -DOTA-TOC PET, whereas in patients with NET,  $^{68}\text{Ga}$ -DOTA-MG0 PET could have added value when  $^{68}\text{Ga}$ -DOTA-TOC PET is equivocal or negative. In this study,  $^{68}\text{Ga}$ -DOTA-MG0 for detection of CCK<sub>2</sub>/gastrin-positive tumors with PET was evaluated in comparison to  $^{111}\text{In}$ -DOTA-MG0.

DOTA-MG0 could be labeled with  $^{68}\text{Ga}$  with high efficiency, in a one-step reaction, reaching specific activities as high as 30 GBq/ $\mu\text{mol}$ . The labeling mixture was purified by RP-HPLC to remove  $^{68}\text{Ga}$ -colloid as well as unincorporated  $^{68}\text{Ga}$ . After purification, a radiochemical purity of > 99% was obtained. By RP-HPLC purification, the colloid contamination could be removed completely. As a result, this preparation had the same very low level of uptake in liver and spleen as the  $^{111}\text{In}$ -labeled preparation.

Biodistribution studies in BALB/c nude mice with a subcutaneous AR42J tumor showed high tumor uptake of  $^{68}\text{Ga}$ -DOTA-MG0 that was CCK<sub>2</sub>/gastrin receptor mediated.  $^{68}\text{Ga}$ -DOTA-MG0 showed biodistribution characteristics as favorable as those of  $^{111}\text{In}$ -DOTA-MG0. Recently, it has been shown that  $^{68}\text{Ga}$ -labeled DOTA-TATE had a higher affinity for the somatostatin receptor subtype 2 than  $^{111}\text{In}$ -DOTA-TATE.<sup>12</sup> In contrast to this study, there was no difference in affinity or tumor uptake between  $^{nat}\text{In}$ -DOTA-MG0 and  $^{nat}\text{Ga}$ -DOTA-MG0. Remarkably, the kidney retention of  $^{68}\text{Ga}$ -DOTA-MG0 is two times higher compared to that of  $^{111}\text{In}$ -DOTA-MG0. The explanation for the higher kidney retention of the  $^{68}\text{Ga}$ -labeled compounds remains unclear.

In this mouse model, a DOTA-MG0 dose of 0.1  $\mu\text{g}$  resulted in maximal tumor accumulation. Administration of higher peptide doses resulted in partial saturation of the CCK<sub>2</sub>/gastrin receptor, leading to lower accumulation of the tracer in the tumor. Thus, high specific activities of the tracer are required to administer a sufficient activity dose for imaging. These results are in line with previous studies showing the importance of high specific activities of radiolabeled peptides and the influence of the peptide dose on tracer characterization *in vitro*<sup>13</sup> and *in vivo*.<sup>14–16</sup> Subcutaneous AR42J tumors in BALB/c nude mice were clearly visualized by PET imaging after intravenous injection of  $^{68}\text{Ga}$ -labeled DOTA-MG0. Peritoneal tumors were visualized despite high kidney uptake of the tracers, and even tumors that were in close proximity to the kidneys were visible on PET images. The high positron range of  $^{68}\text{Ga}$  causes some blurring of the PET images, especially around the kidneys, where high uptake is observed. In a clinical setting, the positron range will be of less importance because under these circumstances, the resolution of the scanner will be the limiting factor. Inflammation observed macroscopically in one mouse was not visualized in the PET images. These data suggest that  $^{68}\text{Ga}$ -DOTA-MG0 is specific for imaging CCK<sub>2</sub>/gastrin receptor-expressing tumors. However, this issue should be examined in more detail.

Radiolabeled DOTA-MG0 (DOTA-DGlu-(Glu)<sub>5</sub>-mini-gastrin) showed relatively high kidney uptake. A previous study showed only limited CCK<sub>2</sub>/gastrin receptor messenger ribonucleic acid expression in murine kidneys as determined by reverse transcriptase–polymerase chain reaction.<sup>17</sup> The biodistribution study showed that the renal uptake of radiolabeled MG0 could not be blocked with an excess unlabeled DOTA-(His)<sub>2</sub>-minigastrin, indicating that the uptake is not CCK<sub>2</sub>/gastrin receptor mediated. Most likely, the high activity levels in the kidneys are due to tubular reabsorption of the peptide via scavenger receptors.<sup>18,19</sup> However, the renal uptake could be reduced by administration of a high dose of unlabeled DOTA-MG0 as observed in the peptide dose escalation study. A previous study showed that the uptake of <sup>111</sup>In-DTPA-MG0 in the kidneys can be reduced by coadministration of polyglutamic acids.<sup>18</sup> The present data suggest that the 6–glutamic acid sequence in the N-terminus of MG0 is responsible for inhibition of renal uptake in the peptide dose escalation study. Apparently, high doses can mimic the effect of polyglutamic acids. DOTA-(His)<sub>2</sub>-minigastrin does not contain this pentaglutamic acid sequence and would therefore only inhibit CCK<sub>2</sub>/gastrin receptor–mediated uptake. The blocking of kidney uptake by DOTA-MG0 appears not to be CCK<sub>2</sub>/gastrin receptor mediated.

Several minigastrin analogues have been developed and characterized.<sup>20</sup> Reduction of the number of glutamic acids in the amino acid sequence of MG0 resulted in an increased tumor to kidney ratio.<sup>20</sup> However, reduction of the number of glutamic acids also reduced the receptor affinity and/or the metabolic stability. Characterization of these minigastrin analogues labeled with <sup>68</sup>Ga might be needed to select the optimal minigastrin analogue for PET imaging.

## Conclusion

<sup>68</sup>Ga-DOTA-MG0 is a suitable PET tracer for the detection of CCK<sub>2</sub>/gastrin receptor–positive tumors. <sup>68</sup>Ga-DOTA-MG0 showed high uptake in subcutaneous AR42J tumors. Moreover, subcutaneous and peritoneal AR42J tumors were clearly visualized with dedicated microPET after injection of <sup>68</sup>Ga-DOTA-MG0. Clinical studies should be conducted to elucidate the potential of <sup>68</sup>Ga-DOTA-MG0 for PET imaging of MTC and NET.

## Acknowledgments

Financial disclosure of authors: This work was supported by National Institutes of Health grant 1R01 AG 030328-01.

Financial disclosure of reviewers: None reported.

## References

1. Krenning EP, Kwekkeboom DJ, Bakker WH, et al. Somatostatin receptor scintigraphy with [<sup>111</sup>In-DTPA-D-Phe1]- and [<sup>123</sup>I-Tyr3]-octreotide: the Rotterdam experience with more than 1000 patients. *Eur J Nucl Med.* 1993; 20:716–31. [PubMed: 8404961]
2. Modlin IM, Tang LH. Approaches to the diagnosis of gut neuroendocrine tumors: the last word (today). *Gastroenterology.* 1997; 112:583–90. [PubMed: 9024313]
3. Lamberts SW, Bakker WH, Reubi JC, et al. Somatostatin-receptor imaging in the localization of endocrine tumors. *N Engl J Med.* 1990; 323:1246–9. [PubMed: 2170840]
4. Gotthardt M, Behe MP, Beuter D, et al. Improved tumour detection by gastrin receptor scintigraphy in patients with metastasised medullary thyroid carcinoma. *Eur J Nucl Med Mol Imaging.* 2006; 33:1273–9. [PubMed: 16832634]



5. Gotthardt M, Behe MP, Grass J, et al. Added value of gastrin receptor scintigraphy in comparison to somatostatin receptor scintigraphy in patients with carcinoids and other neuroendocrine tumours. *Endocr Relat Cancer*. 2006; 13:1203–11. [PubMed: 17158765]
6. Reubi JC, Waser B. Concomitant expression of several peptide receptors in neuroendocrine tumours: molecular basis for in vivo multireceptor tumour targeting. *Eur J Nucl Med Mol Imaging*. 2003; 30:781–93. [PubMed: 12707737]
7. Gabriel M, Decristoforo C, Kendler D, et al. 68Ga-DOTA-Tyr3-octreotide PET in neuroendocrine tumors: comparison with somatostatin receptor scintigraphy and CT. *J Nucl Med*. 2007; 48:508–18. [PubMed: 17401086]
8. Mather SJ, McKenzie AJ, Sosabowski JK, et al. Selection of radiolabeled gastrin analogs for peptide receptor-targeted radio-nuclide therapy. *J Nucl Med*. 2007; 48:615–22. [PubMed: 17401100]
9. Rosewicz S, Vogt D, Harth N, et al. An amphicine pancreatic cell line: AR42J cells combine exocrine and neuroendocrine properties. *Eur J Cell Biol*. 1992; 59:80–91. [PubMed: 1361433]
10. Christophe J. Pancreatic tumoral cell line AR42J: an amphicine model. *Am J Physiol*. 1994; 266(Pt 1):G963–71. [PubMed: 7517639]
11. Visser EP, Disselhorst JA, Brom M, et al. Spatial resolution and sensitivity of the Inveon small-animal PET scanner. *J Nucl Med*. 2009; 50:139–47. [PubMed: 19139188]
12. Reubi JC, Schar JC, Waser B, et al. Affinity profiles for human somatostatin receptor subtypes SST1-SST5 of somatostatin radio-tracers selected for scintigraphic and radiotherapeutic use. *Eur J Nucl Med*. 2000; 27:273–82. [PubMed: 10774879]
13. Velikyan I, Beyer GJ, Bergstrom-Pettermann E, et al. The importance of high specific radioactivity in the performance of 68Ga-labeled peptide. *Nucl Med Biol*. 2008; 35:529–36. [PubMed: 18589296]
14. Breeman WA, Kwekkeboom DJ, Kooij PP, et al. Effect of dose and specific activity on tissue distribution of indium-111-pentetreotide in rats. *J Nucl Med*. 1995; 36:623–7. [PubMed: 7699456]
15. Kooij PPM, Kwekkeboom DJ, Breeman WAP, et al. The effects of specific activity on tissue distribution of [In-111-DTPA-D-Phe1]-octreotide in humans. *J Nucl Med*. 1994; 35:226.
16. de Jong M, Breeman WA, Bernard BF, et al. Tumour uptake of the radiolabelled somatostatin analogue [DOTA0, TYR3]octreotide is dependent on the peptide amount. *Eur J Nucl Med*. 1999; 26:693–8. [PubMed: 10398816]
17. Lay JM, Jenkins C, Friis-Hansen L, et al. Structure and developmental expression of the mouse CCK-B receptor gene. *Biochem Biophys Res Commun*. 2000; 272:837–42. [PubMed: 10860839]
18. Behe M, Kluge G, Becker W, et al. Use of polyglutamic acids to reduce uptake of radiometal-labeled minigastrin in the kidneys. *J Nucl Med*. 2005; 46:1012–5. [PubMed: 15937313]
19. Vegt E, van Eerd JE, Eek A, et al. Reducing renal uptake of radiolabeled peptides using albumin fragments. *J Nucl Med*. 2008; 49:1506–11. [PubMed: 18703613]
20. Good S, Walter MA, Waser B, et al. Macrocyclic chelator-coupled gastrin-based radiopharmaceuticals for targeting of gastrin receptor-expressing tumours. *Eur J Nucl Med Mol Imaging*. 2008; 35:1868–77. [PubMed: 18509636]

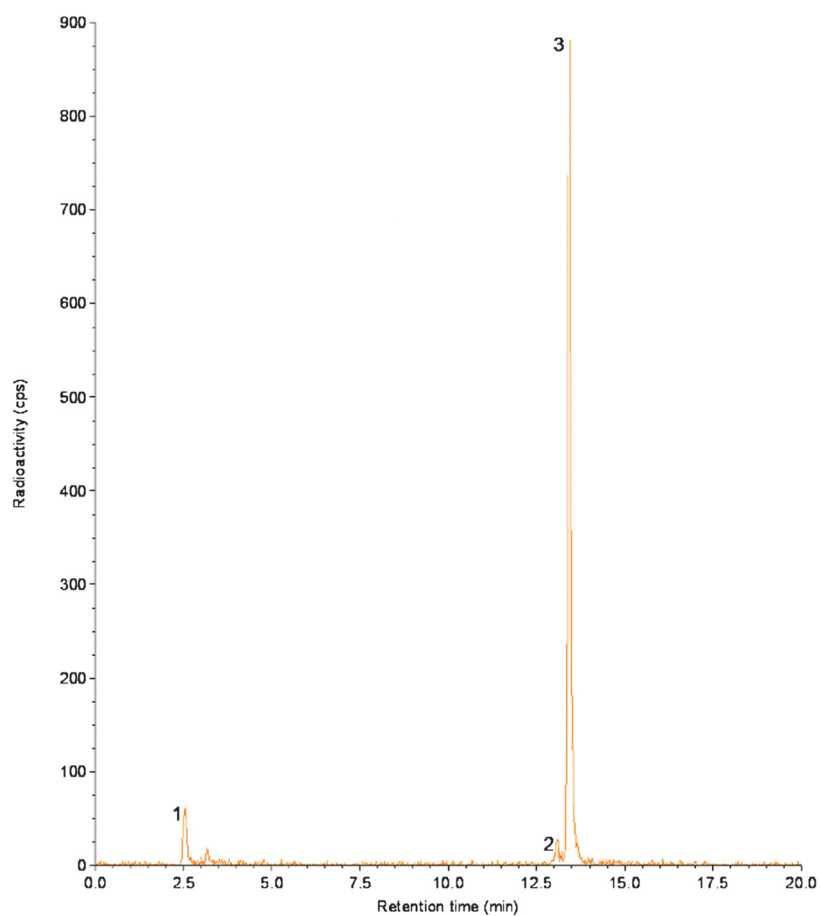


**Figure 1.** HPLC profile of  $^{68}\text{Ga}$ -DOTA-MG0. The first peak represents the unbound  $^{68}\text{Ga}$ , the second peak represents radiolabeled oxidized peptide (retention time 13.2 minutes), and the third peak represents the radiolabeled peptide (retention time 13.5 minutes).

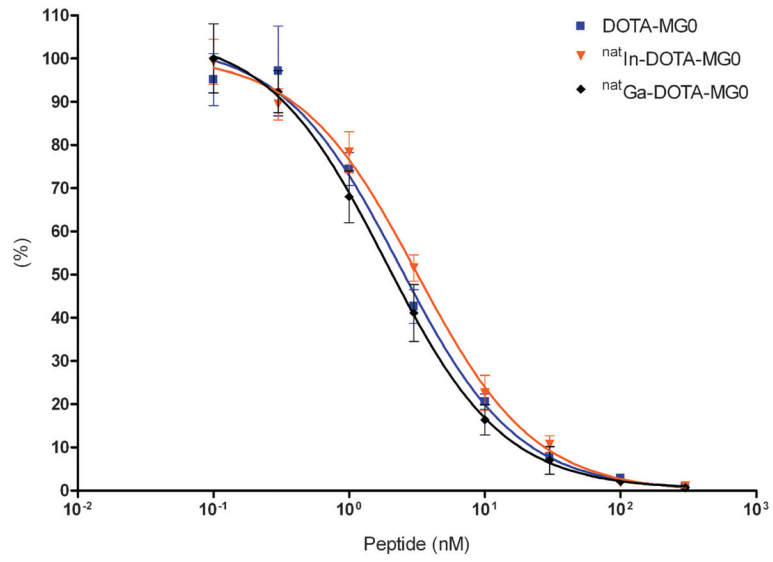


**Figure 2.** Competition binding assay (IC<sub>50</sub>) of DOTA-MG0, <sup>nat</sup>111In-DOTA-MG0, and <sup>nat</sup>67Ga-DOTA-MG0 in AR42J cells. <sup>111</sup>In-DOTA-MG0 was used as a tracer.

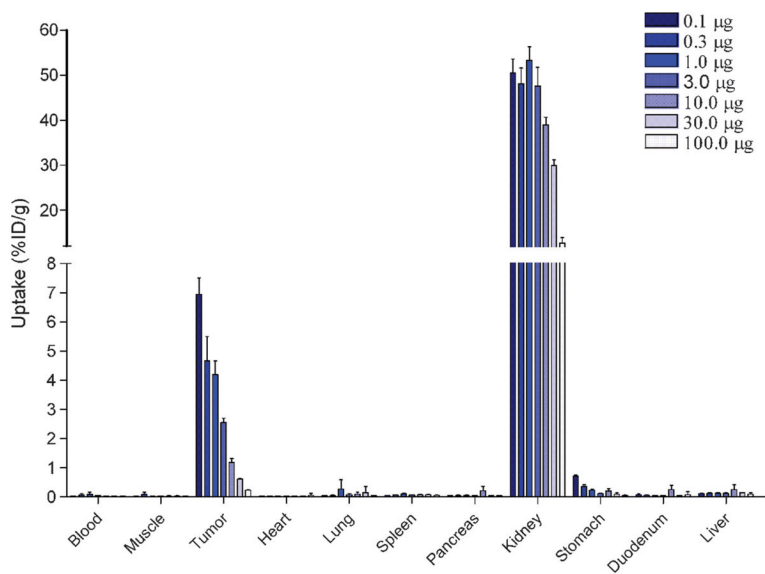


**Figure 3.** Peptide dose escalation study of  $^{111}\text{In}$ -DOTA-MG0 in BALB/c nude mice with subcutaneous AR42J tumors. Mice were injected intravenously with 370 kBq  $^{111}\text{In}$ -DOTA-MG0 and were coinjected with various amounts of unlabeled DOTA-MG0, resulting in final peptide doses ranging from 0.1 to 100.0  $\mu\text{g}$ . Values are expressed as percent injected dose per gram tissue ( $n = 5$  mice). Mice were dissected 1 hour after injection.

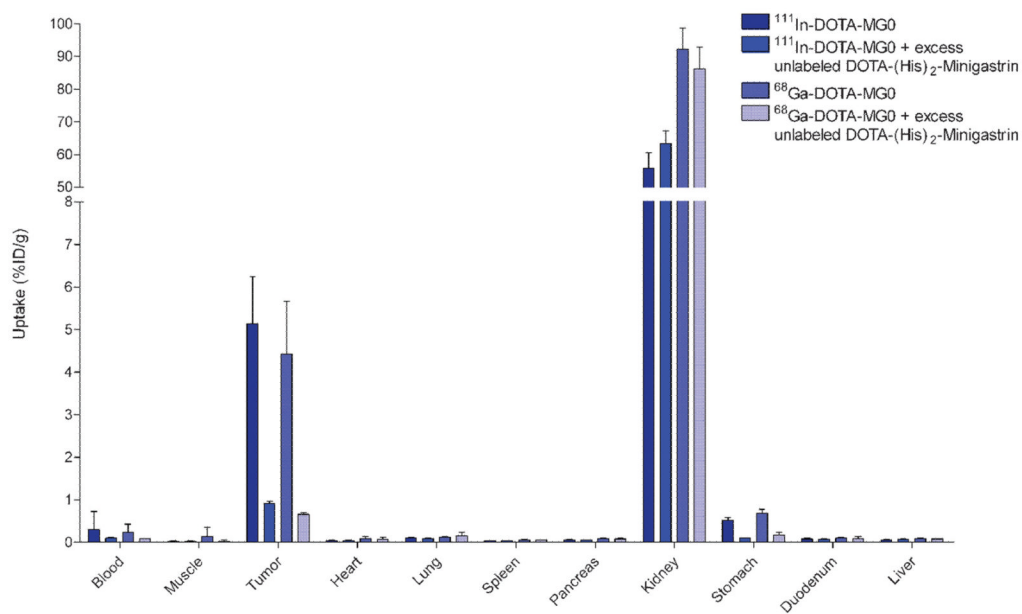


**Figure 4.** Biodistribution of  $^{111}\text{In}$ -DOTA-MG0 and  $^{68}\text{Ga}$ -DOTA-MG0 in BALB/c nude mice with subcutaneous AR42J tumors. Values are expressed as percent injected dose per gram tissue ( $n = 5$  mice). Blocking was performed by coinjection of a 100-fold excess of unlabeled DOTA-(His)<sub>2</sub>-minigastrin ( $n = 3$ ). Mice were dissected 1 hour after injection.

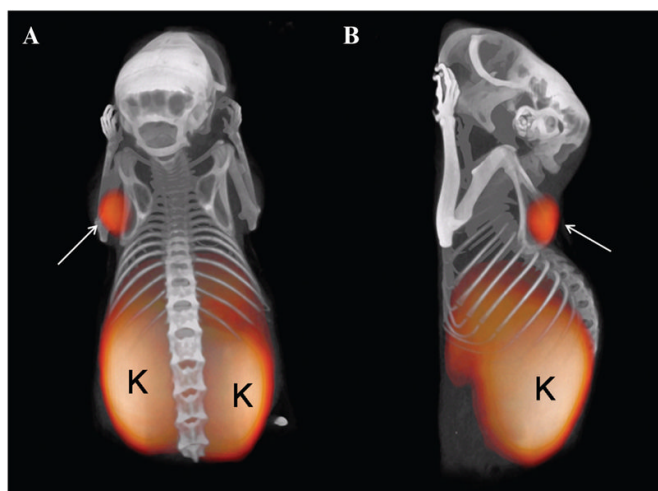


**Figure 5.** Ventral (A) and lateral (B) views of a maximum intensity projection of a BALB/c nude mouse with a subcutaneous AR42J tumor 1 hour after injection of  $^{68}\text{Ga}$ -DOTA-MG0. Tumor (*arrow*) and kidneys (K) are clearly visible. The PET image was fused with CT for anatomic correlation.

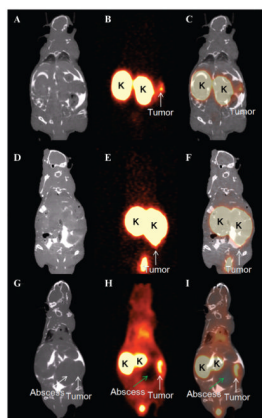


**Figure 6.** Coronal slices of PET images (B, E, H) of three mice with intraperitoneal tumors after injection with  $^{68}\text{Ga}$ -DOTA-MG0. PET images were acquired 1 hour postinjection. CT images (A, D, G) were acquired (after intraperitoneal injection of ioiversol [Optiray 300]) and fused with the PET images (C, F, I) for anatomic correlation. Tumors are clearly visible (*white arrow*), and the kidneys (K) exhibit high uptake of  $^{68}\text{Ga}$ -DOTA-MG0. The abscess (*green arrow*) present in the abdomen of one mouse (G–I) showed no uptake of  $^{68}\text{Ga}$ -labeled MG0. Images were acquired 28 to 35 days after tumor inoculation.

**Table 1**Structure of DOTA-Minigastrin and DOTA-(His)<sub>2</sub>-Minigastrin

Peptide	Amino Acid Sequence	Molecular Weight (Da)
DOTA-minigastrin (DOTA-MG0)	DOTA-Dglu-(Glu) <sub>5</sub> -Ala-Tyr-Gly-Trp-Met-Asp-Phe-NH <sub>2</sub>	2,112.5
DOTA-(His) <sub>2</sub> -minigastrin	DOTA-His-His-Glu-Ala-Tyr-Gly-Trp-Met-Asp-Phe-NH <sub>2</sub>	1,677.8

DOTA = 1,4,7,10-tetraacetic acid.